Quantum Chemical and Molecular Dynamics Study of the Coordination of Th(IV) in Aqueous Solvent

Florent Réal,[†] Michael Trumm,[‡] Valérie Vallet,*[,†] Bernd Schimmelpfennig,[‡] Michel Masella,[¶] and Jean-Pierre Flament[†]

Université Lille 1 (Sciences et Technologies), Laboratoire PhLAM, CNRS UMR 8523, CERLA, CNRS FR 2416, Bât P5, F-59655 Villeneuve d'Ascq Cedex, France, Institut für Nukleare Entsorgung (INE), Karlsruhe Institute of Technology (KIT), Postfach 3640, D-76021 Karlsruhe, Germany, and Laboratoire de Chimie du Vivant, Service d'ingénierie moléculaire des protéines, Institut de biologie et de technologies de Saclay, CEA Saclay, F-91191 Gif sur Yvette Cedex, France

Received: August 25, 2010; Revised Manuscript Received: October 11, 2010

In this work, we investigate the solvation of tetravalent thorium Th(IV) in aqueous solution using classical molecular dynamics simulations at the 10 ns scale and based on polarizable force-field approaches, which treat explicitly the covalent character of the metal−water interaction (and its inherent cooperative character). We have carried out a thorough analysis of the accuracy of the ab initio data that we used to adjust the force-field parameters. In particular, we show that large atomic basis sets combined with wave function-based methods (such as the MP2 level) have to be preferred to density functional theory when investigating Th(IV)/water aggregates in gas phase. The information extracted from trajectories in solution shows a well-structured Th(IV) first hydration shell formed of 8.25 ± 0.2 water molecules and located at about 2.45 ± 0.02 Å and a second shell of 17.5 ± 0.5 water molecules at about 4.75 Å. Concerning the first hydration sphere, our results correspond to the lower bounds of experimental estimates (which range from 8 to 12.7); however, they are in very good agreement with the average of existing experimental data, 2.45 ± 0.02 Å. All our results demonstrate the predictable character of the proposed approach, as well as the need of accounting explicitly for the cooperative character of charge-transfer phenomena affecting the Th(IV)/water interaction to build up reliable and accurate force-field approaches devoted to such studies.

Introduction

Fundamental questions to aqueous chemistry of lanthanide and actinide ions are the structures of the solvated ions, the evolution of the coordination with the type and number of ligands present in the first coordination sphere, as well as the dynamics of the first coordination spheres. Such basic information is highly relevant to the understanding of the separation of the radionuclides and their behavior and transport in the geosphere.[1] These questions can be addressed using various spectroscopy techniques, such as X-ray absorption spectroscopy or nuclear magnetic resonance (NMR) spectroscopy.[2,3] Direct structural and dynamics information can also be obtained with computational chemistry.[2,3]

Theoretical studies of solvated lanthanide and actinide ions are of particular interest as noticeable uncertainties may affect the analysis of experimental data. For instance, several experimental studies discussing the structure of the hydrated thorium(IV) (in highly acidic conditions to avoid the formation of hydrolyzed complexes) have been reported. However, their conclusions concerning the thorium(IV) hydration number are controversial, because it seems to depend not only on the concentration of the solution but also on the counterions present in the solution. EXAFS analyses indicated hydration numbers of 9−11 (Moll et al.)[4−6] and 11.6−12.7 (Rothe et al.)[7] with a Th−O distance of about 2.45 Å. A large-angle X-ray scattering (LAXS) analysis suggested 8.2 ± 0.4 at a distance of 2.49 Å.[8,9] NMR measurements indicated 9.1 water molecules in the first coordination sphere.[10] Part of the discrepancies between the fitted hydration numbers in X-ray absorption spectroscopy is related to the intrinsic uncertainty of this parameter of 10−20%, and its strong correlation to the S_0^2 amplitude prefactor the value of which can vary from 0.8 to 1. Only one crystal structure containing a fully hydrated thorium(IV) ion has been reported, $[Th(H_2O)_{10}]Br_4$, with a mean Th−O bond distance of 2.498 Å in a dicapped square antiprismatic configuration.[11] The hydration of thorium(IV) has also been studied by Tsushima et al.,[12] using DFT (B3LYP) calculations with a PCM solvent model, predicting a hydration number of nine with a distance of 2.47 Å. Yang et al.[13,14] have also performed molecular dynamics simulations using a nonpolarizable force-field. They concluded that thorium binds 9−10 water molecules in the first shell at a distance of 2.54 Å, a distance significantly longer than the experimental values averaged to 2.45 ± 0.02 Å.

Our objective is to shed further light on the scattered experimental and theoretical studies, by providing an accurate theoretical model of hydrated thorium. There are various levels of refinement in the theoretical molecular models that we will now review to underline the advantages and shortcomings of each model and to justify our theoretical approach.

Starting with quantum chemical models, the solvated cluster approach treats the ion and its first hydration shells with quantum chemical methods and the solvent is described by a polarizable dielectric continuum. In the simplest models, such as the Born approximation, the solute is enclosed in a sphere and the solvent

* To whom correspondence should be addressed. E-mail: valerie.vallet@univ-lille1.fr. Phone: +33 3 20 33 59 85. Fax: +33 3 20 43 70 20.
[†] Université Lille1 - CNRS.
[‡] Karlsruhe Institute of Technology.
[¶] CEA Saclay.

10.1021/jp108061s
Published on Web 11/11/2010

effect can be calculated directly from a simple formula.[15] In more advanced models, the cavity has a shape that is adapted to the geometrical form of the solute. The original ansatz used in the shape-adapted conductor-like polarizable continuum model (CPCM)[16] was to associate individual spheres to all atoms in the solute, but later the idea of united atoms (UA0)[17] was introduced, where one spherical cavity is used for compound systems such as water. However, it has recently been shown that the choice of the cavity shape can lead to uncertainties of 2−5 kcal mol^{-1} for the calculation of the relative stabilities of the hydrated uranyl(VI) ions, $[UO_2(H_2O)_n]^{2+}$, $n = 4, 5, 6$.[18,19] Such large deviations alter the confidence in polarizable continuum models and motivates the development of other solvation models, which treat the solvent molecules explicitly and account for the stochastic dynamics.

A way to extend the solvation model is to treat more solvation shells at the quantum chemical (QM) level with the density functional theory (DFT) within the Car−Parrinello molecular dynamics theory[20] as done by Bühl and co-workers (see ref 21 and references therein). However, various theoretical benchmark studies have shown that the currently available exchange correlation functionals that rely on either the local density approximation (LDA) or the generalized gradient approximation (GGA) functionals consistently overestimate the binding energies of various ligands with metal ions, let it be transition metal ions, lanthanide, or actinides.[18,22−27] Only the newly developed meta-GGA functionals (M06 family)[28] seem to yield more accurate binding energies, at least in the case of uranyl(VI), but they are computationally too expensive to be used in Car−Parrinello molecular dynamics simulations.

Computational efficiency might be improved with hybrid quantum chemical/molecular mechanical approaches (QM/MM) in which the first hydration shells are treated at the quantum mechanical level and the more distant ones with classical force-field parameters. Rode et al. have recently applied this modeling scheme to hydrated lanthanide and actinide ions,[29,30] using Hartree−Fock theory to describe the first hydration shell (for the QM part) and a flexible nonpolarizable water model for the MM part. If the QM region is sufficiently large, including, for instance, the first two hydration spheres,[30] one can neglect the interactions between the solute and the solvent molecules of the MM part, thus avoiding the parametrization of the solute−solvent force-field parameters. A first limitation of Rode's modeling scheme is the use of Hartree−Fock theory, which might not be the most accurate ab initio method to describe the electronic structure of molecular complexes with a large number of electrons, such as metal complexes. This will be discussed further in the section on the Ab Initio Calculations of the Th(IV)/Water Dimer Interaction. The second limitation is the same as encountered in Car−Parrinello simulations: the computational cost of the QM or QM/MM calculation at each time step does not allow for simulation times longer than some 10 ps. This might not be long enough to reliably sample the complete phase space of the system. To generate statistically representative structures of a solvated system, it is usually inferred that the simulation time span should be by several orders of magnitude greater than the dielectric relaxation time of the pure solvent, that is about 5−10 ps in the case of water at 298 K.[31−33]

Purely molecular mechanical approaches are computationally very efficient since the intra- and intermolecular interactions are computed with classical force-fields. This enables simulations that extend to much longer time-scales of several tens or hundreds of nanoseconds. The reliability of MM approaches strictly depends not only on the physical interactions the force-fields account for, but also on the accuracy of the parameters that enter the analytical formula of each contribution to the interaction energy. The first MM solvation studies on actinide ions used simple force-fields, which include electrostatic, repulsive, and dispersive contributions determined in a semiempirical way; see, for instance, the work of Guilbaud and Wipff[34] and Hutschka et al.[35] on the hydration of uranyl(VI) or that of Yang and Bursten[36] on curium(III). However, in the presence of charged ions, the ligands and/or the solvent molecules are polarized, an effect that has to be included in a force-field. Furthermore, depending on the ion, the ion−ligand or ion−solvent interaction may have partial covalent character, which has also to be taken into account in a force-field, as pointed out by Hemmingsen et al.[37] and Clavaguéra-Sarrio et al.[38] in the case of uranyl(VI). The importance of both polarization and charge-transfer effects in the determination of the coordination and dynamics of the hydrated complexes was demonstrated by Clavaguéra et al.[39,40] for gadolinium(III) and by Hagberg et al.[41,42] for the hydrated uranyl(VI) and curium(III) complexes. Galbis et al.[43] have also developed a polarizable force-field for californium(III). These recent works differ not only by the choice of the analytical expansions for the interaction energies, but also by the choice and level of theory used in the ab initio data to which the force-field parameters are adjusted. Hagberg et al.[41,42] extracted all information from the metal−water curve interaction computed with relativistic all-electron multiconfigurational level of theory followed by perturbation theory (CASSCF/CASPT2) with triple-ζ quality atomic basis sets. Galbis et al.[43] used relativistic energy-consistent 5f-in-core ab initio pseudopotentials (PP) with quite small atomic basis sets (double-ζ quality). They used either Møller−Plesset second-order perturbation theory (MP2) or density functional theory with the BP86 functional to compute the potential energy surfaces of one cation and a variable set of water molecules, by scanning the release of one water molecule from the first hydration shell. The large differences observed between the computed MP2 and BP86 binding energies, a priori not corrected for basis set superposition errors (BSSE), are not surprising since most exchange-correlation functionals have been shown to bias the metal−ligand binding energies. While MP2 should be considered as more accurate, the BP86 dynamics were found to yield extended X-ray absorption spectra (EXAFS) that are in better agreement with experiment than the MP2 ones. This raises the question of the accuracy of the reference ab initio data and the predictability of their force-field parameters.

This overview of previous works points out the importance of treating simultaneously with the highest accuracy and in the most balanced way both the interactions among the solvent molecules and those between the solute and the solvent. The present study is our first attempt to develop highly accurate force-field models for the dynamics simulations of hydrated actinide complexes. The force-field model includes all important physical effects for the description of the water solvent itself but also of the metal−solvent interaction, such as polarization effects and the covalent character of the metal-solvent bonds. The force-field parameters will be derived from the high-level ab initio data, namely the polarizabilities, interaction energies for various actinide-solvent geometries, and binding/dissociation energies of various hydrated clusters. The details of the force-field model, the reference ab initio data, as well as the approach for adjusting the parameters of the force-field model are presented in Theoretical Details. The Results and Discussion discusses the accuracy of ab initio reference data, and the results

of the dynamics simulations. The results are discussed in the light of the published experimental data.

Theoretical Details

Classical molecular dynamics simulations of hydrated ions require accurate parameters based on ab initio data to describe the pair-interactions occurring between the solvent molecules, the solvent molecules and the charged species, as well as many-body or multicenter interactions. All the parameters described in the previous section were adjusted without using any experimental data, but solely on highly accurate ab initio calculations.

Ab initio Quantum Mechanical Reference Calculations. As shown for closed-shell actinide complexes,[44] spin−orbit coupling has an overall negligible effect on geometries and binding energies of such systems. Hence, we perform all our ab initio computations on thorium/water systems in the scalar-relativistic framework, using the second-order Douglas−Kroll−Hess Hamiltonian.[45,46] All-electron atomic natural orbitals relativistic with core correlation (ANO-RCC) basis sets optimized by Roos et al.[47,48] with quadruple-ζ quality were used to describe all atoms. This corresponds to (27s24p18p14d6g3h)/[10s9p7d5f3g2h], (14s9p4d3f)/[5s4p3d2f], (8s4p3d)/[4s3p2d] contraction schemes for Th, O, and H, respectively.

To decide on the appropriate quantum chemical level required to accurately compute the binding energy (BE) of $Th^{4+}-H_2O$, we compared several levels of theory either within the density functional theory (DFT) framework with a pure GGA functional (BP86[49−53]), a standard hybrid functional (B3LYP[49,50,54,55]) and a set of meta-GGA functionals, namely the recently developed M06 family,[28] or with correlated wave function-based methods (WFT), namely MP2, coupled-cluster singles and doubles with perturbative triples, CCSD(T),[56] and the size-extensive Davidson[57] corrected multireference configuration interaction method (MRCI+DC).[58,59] These calculations were carried out using the MOLPRO[60] and MOLCAS[61] quantum chemistry packages. The computed BEs were corrected for basis set superposition errors (BSSE) with the standard counterpoise method.[62] In the correlated WFT calculations, the 1s oxygen atomic orbitals, as well as the 5d and lower energy thorium orbitals are kept frozen.

To define the Th/water model parameters, we computed the ab initio $Th^{4+}-H_2O$ dissociation energy curve, approaching the water molecule from the oxygen side (C_{2v} geometry). Anticipating our results, the analysis of the $Th^{4+}-H_2O$ wave function along the dissociation path shows that electron transfer between the Th^{4+} ion and the H_2O molecule occurs at 3.25 Å leading to the $Th^{3+}\cdots H_2O^+$ and $Th^{2+}\cdots H_2O^{2+}$ dissociation limits, which lie lower in energy than the $Th^{4+}\cdots H_2O$ one. These changes of electronic configuration cause all single-reference methods to fail in the crossing region. The $Th^{4+}\cdots H_2O$ pair-potential can thus only be computed by multireference WFT methods to describe both Th^{4+}/H_2O and Th^{3+}/H_2O^+ electronic configurations.

The complete active space (CAS) SCF method was used to generate molecular orbitals and reference functions for subsequent MRCI+DC or multistate-CASPT2 calculations of the dynamic electron correlation. The active orbital space includes the highest nonbonding π orbital of the water molecule and the thorium 5f and 6d orbitals. This active space can describe the closed-shell wave function ($\pi^2 5f^0$ configuration) and the other electronic states corresponding to the $\pi^1 5f^1$ and $\pi^1 6d^1$ configurations. We shall mention here that higher excitations yielding to the $Th^{2+}\cdots H_2O^{2+}$ dissociated systems may appear at low energies toward the dissociation limit and cross the Th^{4+}/H_2O and Th^{3+}/H_2O^+ states, leading to convergence problem in the CASSCF and post-CASSCF steps. Therefore, the excitation level was restricted in the CAS space in such a way that the 5f and 6d can accept at most one electron. Our assumption that the $\pi^1 6d^1$ states are not coupled to the $\pi^2 5f^0$ and $\pi^1 5f^1$ states due to the atomic character of the orbitals was confirmed by test calculations. We thus ignored the $\pi^1 6d^1$ in the MRCI + DC calculations.

The potential curves of the open-shell $\pi^1 5f^1$ states should be splitted by spin−orbit coupling. However, since spin−orbit coupling affects the potential curve of Th^{4+}/H_2O only to second-order of perturbation theory, it is possible to disregard spin−orbit coupling for the open-shell dissociating curves when diabatizing the Th^{4+}/H_2O one.

To further analyze the Th/water interaction, we carried out an energy decomposition of the $Th^{4+}-H_2O$ hetero dimer BE according to the reduced variation space (RVS) scheme[66] as implemented in Gamess-US.[67] Such a scheme allows the decomposition of the dimer interaction energy into components of electrostatics, exchange repulsion, polarization, and charge-transfer. The computations were performed at the Hartree−Fock level, using relativistic energy-consistent ab initio small-core pseudopotentials (PP)[68] together with the segmented contracted (14s13p10d8f1g)/[10s9p5d4f1g] basis set[69] for thorium and aug-cc-pVTZ basis sets for water.[70]

Lastly, we have also investigated in gas phase the $\{[Th(H_2O)_n]^{4+},(H_2O)_{10-n}\}_{n=8,9,10}$ clusters using the MP2 method with the resolution of the identity (RI) approximation,[71,72] and correlating only the valence orbitals as in the $Th^{4+}-H_2O$ case. All the corresponding computations were carried out with the TURBOMOLE package.[73] Thorium, oxygen, and hydrogen were described with the same basis sets as used in the RVS analysis. In addition, we also compute the potential energy curve $\mathbf{C_{9/1}}$ corresponding to the dissociation of one water molecule from the ten-coordinated cluster $[Th(H_2O)_{10}]^{4+}$ (for Th/oxygen distances ranging from 2.55 to 8.0 Å). These data will serve as additional references to increase the accuracy of our force-field parameter sets. The computed BEs were corrected for basis set superposition errors (BSSE) with the counterpoise method,[62] considering Th^{4+} and the water clusters $\{(H_2O)_n,(H_2O)_{10-n}\}_{n=8,9,10}$ as fragments. To check the accuracy of the relativistic PP, we have also performed single-point BSSE-corrected MP2 calculations with the MOLPRO package,[60] using here also the relativistic AE description (ANO-RCC basis sets[47,48] for thorium, aug-cc-pVTZ basis sets for water,[70] and the Douglas−Kroll−Hess relativistic Hamiltonian[45,46]) basis sets for MOLPRO calcls.

The TCPEp and RPOL Polarizable Models for Water. Among the available polarizable models of water (see, for instance refs 74−76 and references therein), we considered for the present study the RPOL[77] and TCPEp[78] models, the latter being developed by one of us. While RPOL considers all water atoms as polarizable centers, TCPEp treats water with one polarizable center only, aiming at a computational speed up. In addition, the TCPEp model treats explicitly the hydrogen-bonding interaction, as detailed in the TCPEp Water Model.

The RPOL Water Model. The RPOL water model decomposes the interaction energy into three terms

$$\Delta U = U_{qq'} + U_{pol} + U_{LJ} \quad (1)$$

The first term corresponds to electrostatic Coulomb interaction

$$U_{qq'} = \sum_{ij} \frac{q_i q_j}{r_{ij}} \quad (2)$$

The atomic charges $\{q_i\}$ considered by RPOL lead to a water dipole moment in gas phase of 2.05 D. All oxygen and hydrogen water atoms correspond to polarizable centers in RPOL, their polarizability being 0.425 and 0.135 Å^3 for oxygen and hydrogen, respectively. The atomic-induced dipole moments $\mathbf{p}_i$ obey

$$\mathbf{p}_i = \alpha_i \mathbf{E}_i \quad (3)$$

Here, α_i is the polarizability of atom i, and $\mathbf{E}_i$ the total electric field acting on it

$$\mathbf{E}_i = \mathbf{E}_i^0 + \sum_{i \neq j} \mathbf{T}_{ij} \mathbf{p}_j \quad (4)$$

with $\mathbf{T}_{ij}$ as the dipole tensor[77] and $\mathbf{E}_i^0$ as the electric field acting on i and generated by the static charges $\{q_j\}$ of atoms not belonging to the water molecule containing atom i. Assuming the dipole moments to obey a Born−Oppenheimer regime (they relax instantaneously as the polarizable centers evolve), the polarization energy can be thus expressed as

$$U_{pol} = -\frac{1}{2} \sum_i \mathbf{p}_i \cdot \mathbf{E}_i^0 \quad (5)$$

U_{LJ} is a Lennard-Jones (LJ) potential, which accounts for repulsive and dispersive van der Waals effects

$$U_{LJ} = \sum_{ij} 4\varepsilon_{ij} \left[\left(\frac{\sigma_{ij}}{r_{ij}} \right)^{12} - \left(\frac{\sigma_{ij}}{r_{ij}} \right)^{6} \right] \quad (6)$$

Here, ε_{ij} and σ_{ij} are parameters depending on the atom types.

The TCPEp Water Model. The TCPEp model splits the interaction energy into five terms

$$\Delta U = U_{qq'} + U_{pol} + U_{rep} + U_{rel} + U_{HB} \quad (7)$$

corresponding to the electrostatic Coulomb interaction, and to a polarization, a repulsive, an intramolecular relaxation, and a specific hydrogen bond term, respectively.[79] The repulsive term U_{rep} has a classical additive analytical form

$$U_{rep} = \sum_{i \neq j} A_{ij} \exp(-B_{ij} r_{ij}) \quad (8)$$

In TCPEp, only heavy atoms are considered as polarizable centers. Hence, in the case of water, only its oxygen is considered as a polarizable center with a polarizability of 1.45 Å^3 (note the dipole moment of water in gas phase is 1.85 D for TCPEp). As discussed in our recent paper showing[80] how to combine a polarizable all atoms force-field with a polarizable solvent coarse-grained approach, the TCPEp model allows the induced dipole moments $\mathbf{p}_i$ to reach saturation according to

$$\mathbf{p}_i = \frac{p_{i,sat}}{E_i} L\left(\frac{3\alpha_i E_i}{p_{i,sat}} \right) \mathbf{E}_i \quad (9)$$

where L denotes the Langevin function, $\mathbf{E}_i$ is the total electric field at the atomic polarizable center i, and α_i and $p_{i,sat}$ are, respectively, the isotropic polarizability and the induced dipole saturation value of the latter polarizable center. In the context of "pure" all atoms simulations, it is not obvious to justify the use of such an approach to handle microscopic polarization phenomena. Thus, we chose for the present study sufficiently high saturation values $p_{w,sat}$ and $p_{Th,sat}$, such that eq 9 reduces to the linear form discussed for RPOL. Test calculations indicated that such a linear regime is obtained by considering a saturation value of 12 D for molecular systems involving tetravalent ions like Th(IV).

Unlike RPOL, TCPEp includes a specific hydrogen bond term U_{HB}, which takes into account the anisotropic character of water/water interactions, as well as the cooperative character inherent to water hydrogen bond networks, as shown by quantum mechanical calculations.[81] It corresponds to an anisotropic function

$$U_{HB} = \sum f(r) g(\phi, \psi) \quad (10)$$

Here, the sum runs over all the hydrogen bond pairs, r corresponds to the hydrogen bond length, and f is defined as

$$f(r) = D_{hb} \exp(-(r - r_{hb}^0)^2 / \gamma_r) \quad (11)$$

where r_{hb}^0 is the water dimer equilibrium hydrogen bond length, and D_{hb} and γ_r are assigned respectively to reproduce the water dimer BE (as computed in the complete basis set limit framework,[82] i.e., 5 kcal/mol^{-1}) and the harmonic vibrational frequency corresponding to the ν_{HB} stretching mode.

The most noticeable feature of the function $f(r)$ originates from its cooperative character. If we consider a particular water molecule **w** whose oxygen is involved in a hydrogen bond described by eq 11, D_{hb} and r_{hb}^0 are functions depending on the chemical environment of its hydrogens

$$D_{hb}(R) = d_{hb}(1 + \xi_1 \sum f(R)) \quad (12)$$

$$r_{hb}(R) = r_{hb}(1 - \xi_2 \sum f(R)) \quad (13)$$

The sums run on the two hydrogens of **w**, and R is the length of hydrogen bonds where the latter hydrogens are involved. The parameters ξ_1 and ξ_2 have been adjusted to reproduce the properties of cyclic water trimers (in terms of BEs and geometries).[76,78,79] Lastly, the angular function g is defined according to

$$g(\phi, \psi) = \left(\exp\left(-\frac{(\phi - \phi_{hb})^2}{\gamma_\phi} \right) + \exp\left(-\frac{(\phi + \phi_{hb})^2}{\gamma_\phi} \right) \right) \times \exp\left(-\frac{(\psi - \psi_{hb})^2}{\gamma_\psi} \right) \quad (14)$$

ϕ and ψ angles are defined in Figure 1 (ϕ_{hb} and ψ_{hb} are their corresponding equilibrium values in the water dimer as predicted

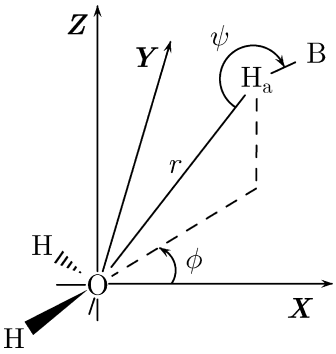

Figure 1. Definition of the geometrical parameters of the term energy U_{HB}. (X, Y, Z) is an orthogonal frame.

by quantum chemical MP2 computations[76]). γ_ϕ and γ_ψ are assigned to reproduce the energy differences among important stationary points of the water dimer potential energy surface (PES).[76,78] The TCPEp parameters used in the present study to describe the interactions among water molecules correspond to those given in ref 83. They were shown to accurately describe the properties of liquid water in ambient conditions such as the water diffusion coefficient and the mean dipole moment per water molecule.

The Ion−Water Model. ***Energy Decomposition of the Ion−Water Interaction.*** To study Th(IV) systems using polarizable force-field approaches, the first key parameter to assign is the Th(IV) atomic electric-dipole polarizability, $\alpha_{Th(IV)}$. The values found in the literature are very scattered, ranging from 1.30 to 2.90 Å^3, and thus cannot be trusted.[84−86] For instance, the value reported in the *Handbook of Atomic Data*,[84] 1.52 Å^3, was derived from variation-perturbation calculations that treat relativistic effects as perturbations, while for such heavy ions relativistic effects play a major role and have thus to be treated at the variational level with a proper relativistic Hamiltonian. Moreover, available experimental values refer to actinide materials and not to the ion in the gas-phase.[85,86] We therefore consider here our own four-component correlated atomic computed value of 1.142 Å^3, which we recently reported,[87] and that is significantly lower than the quoted data from the literature.

The interactions between Th(IV) and water molecules are described by the TCPEp energy terms U_{rep}, $U_{qq'}$ and U_{pol} terms, to which a specific charge-transfer term U_{ct} is added to account for the partial "covalency" of the actinide-water bond. The latter contribution is described by a basic exponential term, as already used by many authors (for instance, Hagberg and co-workers[41,42])

$$U_{ct} = \sum_i D_{ct}^i \exp(-\beta_{ct} r_{Th-i}) \qquad (15)$$

The sum runs over all possible ion/water pairs Th$-i$ and r_{Th-i} corresponds to the Th/oxygen distance. It is well established that the electronic charge-transfer intensity between two chemical entities can be strongly affected by their chemical environment. In other words, the charge-transfer contribution is not an additive quantity (note that the above-mentioned studies by Hagberg et al. concerning uranyl(VI) and curium(III) were performed using a pure additive U_{ct} energy term). One way to account for the cooperative character of charge-transfer phenomena is to consider an approach similar to that of the TCPEp energy term U_{HB}. According to such an approach, the charge-transfer intensity is a linear function of the number N_w of water molecules neighboring the ionic center. Here, we choose to introduce such effects by considering D_{ct}^i as a function with the following analytical form

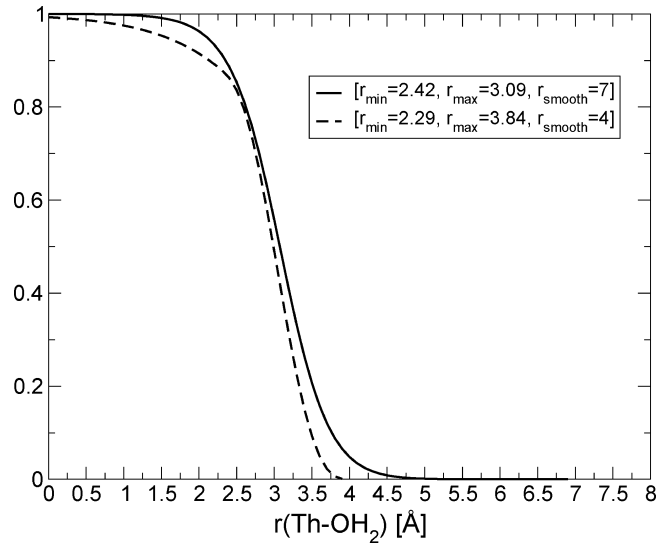

Figure 2. Plots of the functions $F_{ct}^i(r)$ corresponding to $r_{smooth} = 4$ and 7 Å.

$$D_{ct}^i(r) = d_{ct}(1 + \xi_{ct} \sum_{j \neq i} F_{ct}^j(r)) \qquad (16)$$

ξ_{ct} is an adjustable parameter, whereas F_{ct}^j is a function quantifying the incidence of a given water molecule j on the charge-transfer effect taking place between the ion and the water molecule i. If the function F_{ct}^j values are included within 0 and 1, the sum occurring in the latter equation may be considered as providing an estimate of N_w. Many choices are possible for the function F_{ct}^j, such as a Gaussian function of the ion/oxygen water distance r (and centered at the distance characterizing the first hydration shell of the ion). Here, we choose a Fermi-like analytical form

$$F_{ct}^j(r) = \left[\exp\left(2\frac{r - r_{min}}{r_{max} - r_{min}}\right) + 1\right]^{-1} P_5(r) \qquad (17)$$

r is the above distance, and r_{min} and r_{max} are two adjustable parameters ($r_{max} > r_{min}$). The expression includes the well-known five order polynomial switching function P_5,[88] which allows to zero the cooperative incidence of a water molecule whose distance r from the ion is beyond a chosen cutoff value r_{smooth}. Such F_{ct}^j profiles are plotted in Figure 2.

Assigning Th(IV)/Water Energy Term Parameters. To assign the U_{rep}, $U_{qq'}$, U_{pol}, and U_{ct} parameters corresponding to Th(IV)/water interactions (at the exception of the Th(IV) polarizability, the water and thorium saturation dipole values $p_{w,\,sat}$ and $p_{Th,\,sat}$, and the U_{ct} parameter r_{smooth}), we followed an automated two steps parameter adjustment procedure, using the Model-Independent Parameter Estimation (PEST) software package.[89] First, the parameters of the repulsive and charge-transfer terms eqs 8 and 15 are adjusted to reproduce the ab initio $Th^{4+}-H_2O$ dissociation energy curve, approaching the water molecule from the oxygen side in a C_{2v} geometry and keeping its geometry fixed to the one considered in molecular dynamics simulations (see below). Then, these parameters are kept fixed and the second fitting step involves the adjustment of ξ_{ct}, r_{min}, and r_{max},

TABLE 1: Binding Energies of the Water Clusters, ΔE_{water}, in kcal mol^{-1}, Computed with Two Different Quantum Chemical Methods and the RPOL and TCPEp Polarizable Water Models[a]

method	$[Th(H_2O)_8]^{4+},(H_2O)_2$	$[Th(H_2O)_9]^{4+},(H_2O)_1$	$[Th(H_2O)_{10}]^{4+}$
		ΔE_{water}	
B3LYP	50	42	61
MP2	33	26	41
TCPEp	54	49	72
RPOL	68	77	116
		$\widetilde{BE}_{BSSE}$	
MP2	−879	−867	−872
$\mathbf{M}_4^{TCPEp}$	−877	−867	−866
$\mathbf{M}_7^{TCPEp}$	−877	−867	−868
$\mathbf{M}_4^{RPOL}$	−861	−862	−856
$\mathbf{M}_7^{RPOL}$	−864	−864	−861

[a] $\widetilde{BE}_{BSSE}$ energies in kcal mol^{-1} computed at the MP2 level and with the four $\mathbf{M}_{4,7}^{TCPEp/RPOL}$ parameter sets.

which enter the analytical formula of the cooperative charge-transfer effects (see eq 17); they are optimized to reproduce the ab initio MP2 data of the $([Th(H_2O)_n]^{4+},(H_2O)_{10-n})_{n=8,9,10}$ clusters, as well as the potential energy curve $\mathbf{C_{9/1}}$ that corresponds the dissociation of one water molecule from the ten-coordinated cluster $[Th(H_2O)_{10}]^{4+}$. All ab initio reference data concerning the Th(IV)/water dimer and ten-coordinated clusters were computed according to the protocol presented in the ab initio Quantum Mechanical Reference Calculations section.

Concerning the Th(IV)/$(water)_{10}$ clusters, the above-mentioned MP2 data correspond to the BSSE corrected cluster BEs from which the energies ΔE_{water} corresponding to the interaction among the cluster water molecules have been subtracted (the new resulting energy quantity is labeled $\widetilde{BE}_{BSSE}$).

$$\Delta E_{water} = E[(H_2O)_n,(H_2O)_{10-n}] - 10E[H_2O] \quad (18)$$

$$\widetilde{BE}_{BSSE} = BE_{BSSE} - \Delta E_{water} \quad (19)$$

This choice originates from the fact that the RPOL and TCPEp water models and quantum chemical MP2 and DFT methods do not predict the same interaction energies ΔE_{water} for the latter clusters. The differences between models and quantum chemical ΔE_{water}'s varies from 14 to 75 kcal mol^{-1}, see Table 1. Thus, to fit the ion/water parameters, we prefer to consider the "pure" ion/water MP2 data $\widetilde{BE}_{BSSE}$, to prevent artifacts arising from cancellation of errors between water/water and ion/water interaction energies.

Regarding the parameter r_{smooth}, accurate ab initio data concerning Th(IV) interacting with at least two hydration spheres are needed to assign it. However, accurate quantum chemical computations on such large systems are still far from being feasible with the available computational resources. Charge transfer effects among Th and water molecules are mostly expected to be affected by the first hydration shell. Because of their fast decreasing character, the incidence of the second hydration shell is expected to be weak. Accordingly, we consider only two possible values for r_{smooth}: 4 and 7 Å. With such values, the second hydration sphere water molecules (about 20, see Solvated Th(IV) at Ambient Conditions) affect the D_{ct}^i values of the energy term U_{ct} (cf. eq 17) by 0.1 and 10%, respectively.

TABLE 2: Fitted Parameters for the Different Th(IV)/Water Models[a]

	$\mathbf{M}_4^{TCPEp}$	$\mathbf{M}_7^{TCPEp}$	$\mathbf{M}_4^{RPOL}$	$\mathbf{M}_7^{RPOL}$	$\mathbf{M}'^{TCPEp}_4$
A_{ij}	57468		49237		57956
B_{ij}	3.18		2.70		3.15
d_{ct}	527		4759		984
β_{ct}	0.766		0.645		0.690
ξ_{ct}	0.087	0.089	0.057	0.049	0.077
r_{min}	2.23	2.06	2.489	3.224	2.26
r_{max}	3.46	3.24	3.862	3.675	3.93

[a] $\mathbf{M}'^{TCPEp}_4$ is a second set of parameters providing the results as $\mathbf{M}_4^{TCPEp}$ (see text for details). A_{ij}, B_{ij}, and d_{ct} are in kcal mol^{-1}; β_{ct} is in Å^{-1}; ξ_{ct} is unitless; r_{min} and r_{max} are in Å.

According to the above discussions, we define four different parameter sets (labeled $\mathbf{M}_{r_{smooth}}^{water-model}$) corresponding to both the latter r_{smooth} values as well as to the water models RPOL and TCPEp (which differ by the electrostatic charges and polarizabilities of the water atoms). These parameter sets are summarized in Table 2. They are equally able to reproduce the ab initio reference data with a high accuracy, the $Th^{4+}-H_2O$ dimer dissociation curve within 0.1 kcal mol^{-1} and the ten coordinated Th/water system $\widetilde{BE}_{BSSE}$ within less than 4 kcal mol^{-1} (that represents less than 0.5% of the latter $\widetilde{BE}_{BSSE}$). Note that, because of our two steps procedure for assigning the force-field parameters, the parameter sets $\mathbf{M}_{r_{smooth}}^{RPOL/TCPEp}$ lead to the same results concerning the Th(IV)/water dimer system, regardless of the value of r_{smooth}.

Lastly, as the energy terms U_{ct} and U_{rep} are based on similar analytical functions (driven by a distance-decreasing exponential), our least-squares procedure can provide different sets of parameters when considering different initial guesses (and the same fitting convergence criterion). An example of two such close parameter sets are summarized in Table 2 in the case [r_{smooth} = 4 Å, water model = TCPEp]. We performed all the computations discussed below concerning Th(IV)/water systems in gas phase or in solution with both parameter sets; their results only differ by some tenth of percent. This is why we will only discuss in the following the results corresponding to one such parameter set, that is, that labeled $\mathbf{M}_4^{TCPEp}$ in Table 2.

Molecular Dynamics Details. The starting points of the trajectories correspond to the three $\{[Th(H_2O)_n]^{4+},(H_2O)_{10-n}\}_{n=8,9,10}$ Th(IV)/water systems discussed in the ab initio Quantum Mechanical Reference Calculations section, solvated into cubic boxes containing about 1000 water molecules, with periodic boundary conditions. The density of water is set to 1.00 g cm^{-3}. Hence, for both the parameter sets $\mathbf{M}_{r_{smooth}}^{TCPEp}$, we perform three 10 ns MD simulations based on the latter starting points. The trajectories are generated under constant temperature condition (300 K) using the generalized Gaussian moment thermostat,[90] which ensures a canonical ensemble (the thermostat coupling constant was set to 250 fs).

The induced dipole moments are evaluated iteratively with a convergence criterion of 10^{-6} Debye per polarizable center (however, the iterations continue until the greatest difference between two successive iterations of the induced dipole moment for a single polarizable center is smaller than 5×10^{-6} Debye).

Both the electrostatic and polarization interactions are calculated using the Ewald summation technique.[91] The parameter α of the direct term and the vectors $\mathbf{m}$ considered in the reciprocal sum are assigned to meet: $\mathrm{erfc}(\alpha r_c)/r_c < \varepsilon_{Ewald}$ for r_c = 14 Å, and $\exp(-\pi^2|\mathbf{m}|^2/\alpha)/|\mathbf{m}|^2 < \varepsilon_{Ewald}$. In the present study, ε_{Ewald} is set to 10^{-6}.

The equations of motion are solved using an integration scheme based on the multitime-step r-RESPAp procedure,

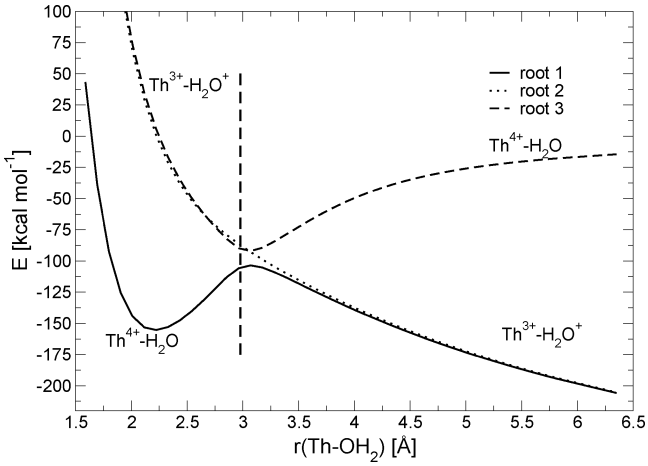

Figure 3. Potential energy profiles computed at the quantum chemical MRCI+DC level of the $[Th/H_2O]^{4+}$ dimer.

developed for polarizable potentials.[88] Two time steps are considered: 1 fs (short-range repulsive, electrostatic, polarization and charge-transfer forces) and 5 fs (for the remaining long-range electrostatic and polarization forces). The water OH bonds and H−H distances are constrained using the RATTLE procedure,[92] so that the OH bond length and the HOH angle are respectively of 0.96 Å and 104.5° along the trajectories. The RATTLE convergence criterion is 10^{-6} Å. The r-RESPAp scheme permits to generate trajectories with a good accuracy: the rate of the energy drifts is from 2 to 3.10^{-3} kcal mol^{-1} ps^{-1} along the trajectories.

Lastly, the statistical ensembles used to compute all the average values discussed in the present study are generated by sampling the trajectories each 500 fs, once an initial equilibration period of 1 ns is achieved (the geometric parameters and energy quantities are then converged and stable). These statistical ensembles are thus made of 16 000 structures.

Results and Discussion

A Quantum Chemical Study of Th(IV)/Water Interactions in Gas Phase. ***Ab initio Study of the Th(IV)/Water Dimer Interaction.*** We plot in Figure 3 the ab initio $Th^{4+}-H_2O$ dissociation energy versus the Th/oxygen distance. The three lowest states of a_1 representation in the C_{2v} symmetry can be diabatically connected in order to extract the purely repulsive potentials of the electronic states corresponding to Th^{3+}/H_2O^+, as well as the relevant bonded pair potential of the Th^{4+}/H_2O system. At longer Th/oxygen distance, the single-reference configuration follows the lowest $Th^{2+}\cdots H_2O^{2+}$ dissociation limit.

The relevant bonded pair potential profile of the Th^{4+}/H_2O system exhibits a global minimum at a Th/oxygen interatomic distance of 2.22 Å. We computed the Th(IV)/water dimer BE at the DFT and WFT level of theory presented in the ab initio Quantum Mechanical Reference Calculations section, taking the latter equilibrium Th/oxygen distance. The BE values are summarized in Table 3. BEs computed with the three correlated WFT methods agree within 1 kcal mol^{-1}. On the contrary, all DFT functionals (BP86, B3LYP, and M06 variants) yield scattered and overestimated BEs by up to 18 kcal mol^{-1}, which represents about 8% of the WFT BEs. These results are in the line of earlier ones showing that GGA, meta-GGA, as well as hybrid functionals have a tendency to overestimate the BEs of actinide ions interacting with different types of ligands.[18,24−26] Although the recently developed meta-GGA M06 family was found to perform better than GGA and hybrid functionals for the solvation of actinyl ions,[27] it is not more accurate in the $Th^{4+}-H_2O$ case. These observations lead us to consider state-of-the art correlated WFT methods as more relevant than available DFT functionals to generate accurate reference data on Th(IV)/water clusters.

Ab Initio Structures and Energies of {$[Th(H_2O)_n]^{4+}$, $(H_2O)_{10-n}$}$_{n=8,9,10}$ Clusters. The gas phase structures and BEs of the {$[Th(H_2O)_n]^{4+}$,$(H_2O)_{10-n}$}$_{n=8,9,10}$ clusters computed at the MP2 level are reported in Table 4. The MP2 Th/oxygen distances are from 0.02 to 0.10 Å shorter than those obtained by Yang et al.[14] with the B3LYP functional for $n = 9$ and 10. The average MP2 Th/oxygen distances is 2.46 ± 0.02 Å in the eight-coordinated isomer, which is in good agreement with the experimental value in solution of 2.45−2.46 Å,[4,6−8,10,93] while the values in the nine- and ten-coordinated water clusters, 2.55 ± 0.03 and 2.55 ± 0.02 Å are somewhat longer. However, as discussed later in Solvated Th(IV) at Ambient Conditions, the distances of the eight- and nine-coordinated forms that are both present in the statistics match the experimental data very well, thus indicating that the solvation effects tend to shorten the thorium−water distances.

MP2 BEs are about −830 ± 15 kcal mol^{-1}, regardless of the cluster and the relativistic framework used (PP or DKH).

TABLE 3: Binding Energies of the Th(IV)/Water Dimer in kcal mol^{-1} at 2.22 Å Computed with Different Multireference and Single Reference Correlated Methods

WFT				DFT				
HF	MP2	CCSD(T)	MRCI+DC	BP86	B3LYP	MX06-HF	MX06-L	MX06−2X
145	155	155	156	173	165	163	167	161

TABLE 4: Binding Energies in kcal mol^{-1} of the $([Th(H_2O)_n]^{4+},(H_2O)_{10-n})_{n=8,9,10}$ Clusters Computed in Gas Phase at the MP2 Level without and with BSSE Correction, Using Either Relativistic All-Electron (AE) Basis Sets or Pseudopotentials (PP)[a]

	$[Th(H_2O)_8]^{4+},(H_2O)_2$	$[Th(H_2O)_9]^{4+},(H_2O)_1$	$[Th(H_2O)_{10}]^{4+}$
$E_{AE/MP2}$	−850	−845	−836
$E_{AE/MP2}$(BSSE)	−842	−838	−828
$E_{PP/MP2}$(BSSE)	−844	−840	−831
r_{Th-O_I}	2.447 (4), 2.483 (4)	2.484, 2.525, 2.527 2.542, 2.559, 2.574 2.576, 2.578, 2.592	2.519 (2), 2.548 (4) 2.558 (2), 2.588 (2)
$r_{Th-O_{II}}$	4.269 (2)	4.418	

[a] r_{Th-O_I} and $r_{Th-O_{II}}$; Th/oxygen distances in angstroms, corresponding respectively to water molecules of the Th(IV) first and second hydration sphere.

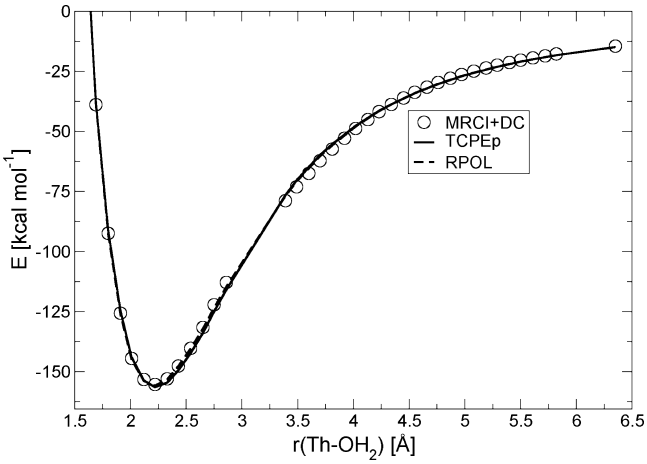

Figure 4. Comparison of the $Th^{4+}-H_2O$ interaction energy profiles computed from the quantum chemical MRCI+DC method (circles), and the TCPEp-based (plain line) and RPOL-based (dashed line) models.

BSSE corrections to the BEs amount to about 7−8 kcal mol^{-1} for all complexes. Even though their relative magnitude is small (it represents about 1% of the total BEs), these corrections have to be accounted for to ensure the highest accuracy of our reference ab initio data. It is noteworthy that BSSE corrected PP BEs agree within less than 3 kcal mol^{-1} with the all-electron ones. This demonstrates that PPs achieve the same accuracy as all-electron relativistic calculations.

Our MP2 BEs indicate that the eight-coordinated cluster, $[Th(H_2O)_8]^{4+}$,$(H_2O)_2$, and the ten-coordinated one $[Th(H_2O)_{10}]^{4+}$ are respectively the most and the least stable in gas phase. Yang et al.[13] reported the same trends at the B3LYP level: the relative energies among the Th/water clusters agree within less than 2 kcal mol^{-1} with our MP2 data. However, Yang's B3LYP BEs (−820, −815, −805 kcal mol^{-1} for $n = 8, 9, 10$, respectively[13]) are at least 25 kcal mol^{-1} higher than our MP2 values (−842, −838, −828 kcal mol^{-1}). The discrepancies between DFT and MP2 energy results observed in the case of hydrated clusters are opposite in sign from those observed in the Th(IV)/water dimer case. As suggested by Ciupka et al.,[94] this may originate from the DFT overestimation of the repulsion among the water molecules belonging to first hydration spheres of ions. Indeed the values ΔE_{water} computed at the DFT level (B3LYP) are 20, 16, and 17 kcal mol^{-1} larger than the corresponding MP2 values for $n = 8, 9, 10$, respectively (See Table 1). We would like to add at this point that the differences between DFT- and WFT-based calculations for these complexes as well as for the Th(IV)/water heterodimer do not forfeit the possibility to derive a force-field that is capable to reproduce several properties in agreement with experiment. Nevertheless, it is our strong opinion that state-of-the-art WFT data should be used to develop a new force-field as only such an approach will allow rigorous assessment of its quality.

Force-Fields Reliability in Gas Phase. ***Th(IV)/Water Dimer Properties.*** As mentioned in Ion−Water Model, the four sets of parameters $\mathbf{M}_{r_{smooth}}^{RPOL/TCPEp}$ are able to reproduce the quantum chemical MRCI+DC dissociation curve of the $Th^{4+}-H_2O$ dimer within 0.1 kcal mol^{-1}. The quality of our models may be assessed in Figure 4, where we plot the quantum chemical curve profile, as well as those corresponding to the models $\mathbf{M}_4^{RPOL}$ and $\mathbf{M}_4^{TCPEp}$, which differ by the considered water model only (note that $\mathbf{M}_7^{RPOL/TCPEp}$ profiles are not drawn in Figure 4 as they superimpose on the $\mathbf{M}_4^{RPOL/TCPEp}$ ones).

The RPOL and TCPEp water models differ by the set of atomic electrostatic charges and polarizabilities. Hence, even if the above $Th^{4+}-H_2O$ dissociation curves based on these models and quantum methods are very close, such an agreement is not expected for the comparable model/quantum energy components (i.e., the components $U_{qq'}$, U_{pol}, and U_{ct}). In Figure 5, we compare the latter energy components computed from the $\mathbf{M}_4^{RPOL}$ and $\mathbf{M}_4^{TCPEp}$ models along the $Th^{4+}-H_2O$ dissociation curve, as well as those computed from the quantum chemical HF RVS energy decomposition analysis presented in the *Ab initio* Quantum Mechanical Reference Calculations section. All the components computed from the quantum chemical and model approaches significantly differ from each other for distances smaller than 2 Å, a domain that is not explored during the molecular dynamics simulations of Th(IV) in solution. For distances greater than 6 Å, all the quantum chemical and models components have the same asymptotic behavior. Lastly, in the critical range lying within 2 and 6 Å, we note that the TCPEp and quantum electrostatic, polarization, and charge-transfer components agree within about 5 kcal mol^{-1}. The RPOL electrostatic component also agrees with the quantum chemical and TCPEp ones. However, the RPOL polarization and charge-transfer components differ significantly from their quantum chemical and TCPEp counterparts from 40 to 70 kcal mol^{-1} (the magnitude of the RPOL polarization component being smaller than the charge-transfer one). These errors compensate each other, resulting in a fair agreement of the RPOL total energies with the quantum chemical ones. The fact that the polarization component in RPOL is twice as small as in TCPEp originates from the smaller water polarizability, 0.70 $Å^3$ as compared to the TCPEp one, 1.45 $Å^3$ (note that the latter value and the TCPEp water dipole moment in gas phase are consistent with experiment.[83])

Hence, the agreement between the TCPEp-based and quantum chemical results for all the energy components discussed above demonstrates that the accuracy of the Th(IV)/water model depends strongly on the quality of the model description of the gas phase water electrostatic properties, a requirement that the RPOL water model does not appear to meet.

Ten-Coordinated Th(IV)/Water Clusters. The reference MP2 and fitted cluster energies $\tilde{B}E_{BSSE}$ for the four models, $\mathbf{M}_{4,7}^{RPOL/TCPEp}$, are reported in Table 1. While the TCPEp parameter sets reproduce the quantum chemical values with a maximum error of 6 kcal mol^{-1}, the RPOL parameter sets display deviations up to three times larger (18 kcal mol^{-1}). The differences between the two force-field models are more striking in Figure 6, in which the models and MP2 energy profiles $\mathbf{C_{9/1}}$ are displayed. The quantum chemical and TCPEp-based profiles behave monotonically, whereas the RPOL-based profiles present a minimum for Th/oxygen distances included within 3.5 to 4.0 Å and behave exponentially for larger Th/oxygen distances. This particular feature of RPOL-based profiles originates from the strong contribution due to the large charge-transfer parameter d_{ct} for RPOL-based models (1 order of magnitude greater than the TCPEp-based ones), as well as from the fast decay of the functions $F_{ct}^j(r)$ (independent of the r_{smooth} value). Hence, the RPOL water model is clearly not suited to be used in conjunction with our cooperative charge transfer energy term U_{ct} to model Th(IV) water systems of arbitrary size (see also the above discussion concerning the Th(IV)/water dimer). This is the reason why we only consider the TCPEp-based models $\mathbf{M}_{4,7}^{TCPEp}$ to explore the dynamics properties of Th(IV) in aqueous solution, as these models are able to reproduce gas-phase cluster energies with a good accuracy (See Table 1, and Figure 6).

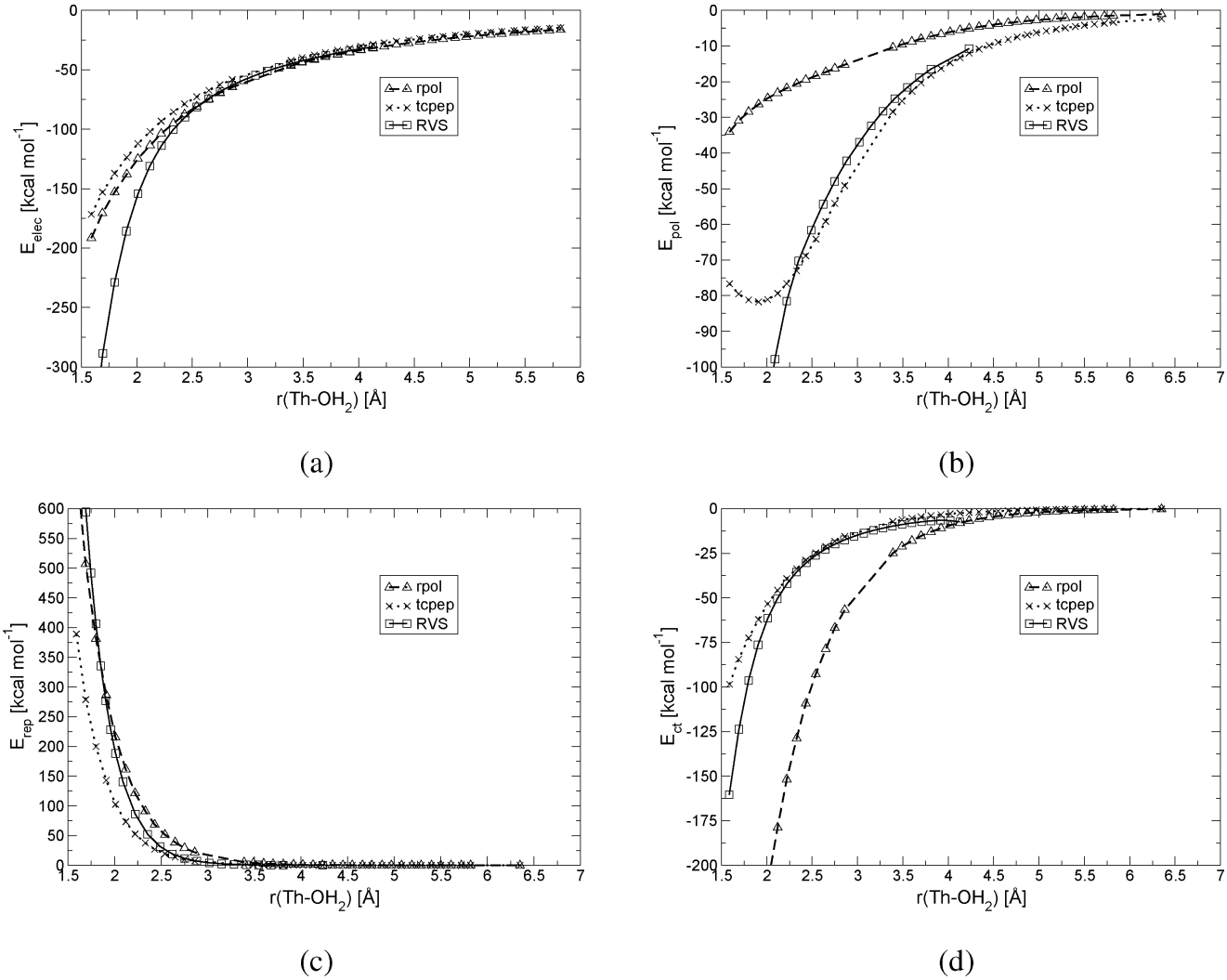

Figure 5. Comparison of the various energy contributions to the Th(IV)/water dimer interaction energy, computed from the RVS energy decomposition analysis (squares), the TCPEp-based (crosses) and RPOL-based (diamonds) models. Electrostatic energy (a), polarization energy (b), repulsion energy (c), and charge-transfer energy (d).

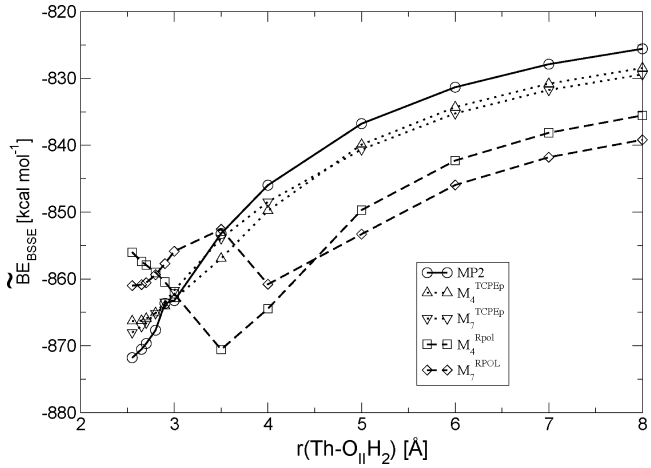

Figure 6. Comparison of $\widetilde{BE}_{BSSE}$ in kcal mol^{-1} for the $\mathbf{C_{9/1}}$ curve corresponding to the dissociation of one water molecule from the ten-coordinated cluster $[Th(H_2O)_{10}]^{4+}$, computed from the quantum chemical MP2 method and the $\mathbf{M}_{4,7}^{TCPEp}$ and $\mathbf{M}_{4,7}^{RPOL}$ models.

When defining the analytical form of the charge-transfer energy term U_{ct}, we assume that the Th(IV)/water charge-transfer phenomenon is not additive. Here, we may note that if we use the raw parameters optimized by considering only the Th(IV)/water dimer quantum chemical data (with the parameters ξ_{ct} zeroed), the TCPEp model would strongly overestimate the BEs of the $\{[Th(H_2O)_n]^{4+},(H_2O)_{10-n}\}_{n=8,9,10}$ hydrated clusters ($\widetilde{BE}_{BSSE}$ = −964, −960, −983 kcal mol^{-1}, respectively) compared to quantum chemical MP2 values ($\widetilde{BE}_{BSSE}$ = −879, −867, −872 kcal mol^{-1}, respectively, See Table 4), by about 100 kcal mol^{-1}. This illustrates how strong cooperative charge-transfer effects are in the Th(IV)/water clusters, effects that have never been accounted for up to now in simulations of large actinide/water systems.

Solvated Th(IV) at Ambient Conditions. For both parameter sets $\mathbf{M}_{4,7}^{TCPEp}$, we generated three 10 ns trajectories, whose starting points correspond to the three hydrated $\{[Th(H_2O)_n]^{4+}, (H_2O)_{10-n}\}_{n=8,9,10}$ clusters. Once the first *n*s achieved, each set of three trajectories evolves similarly, that is, the solvation structure of Th(IV) is the same and the total potential energy along the trajectory differ at most by 1 kcal mol^{-1} (which represents less than 0.01% of the total potential energy).

In Figure 7, we plot the radial distribution functions $g_{Th-O}(r)$ and $g_{Th-H}(r)$ corresponding respectively to the Th/oxygen and Th/hydrogen distances, as well as their integrated profiles, computed along the trajectories $\mathbf{M}_4^{TCPEp}$ and $\mathbf{M}_7^{TCPEp}$. The $g_{Th-O}(r)$'s and $g_{Th-H}(r)$'s are characterized by a narrow peak respectively centered around 2.455 ± 0.015 and 3.14 ± 0.02

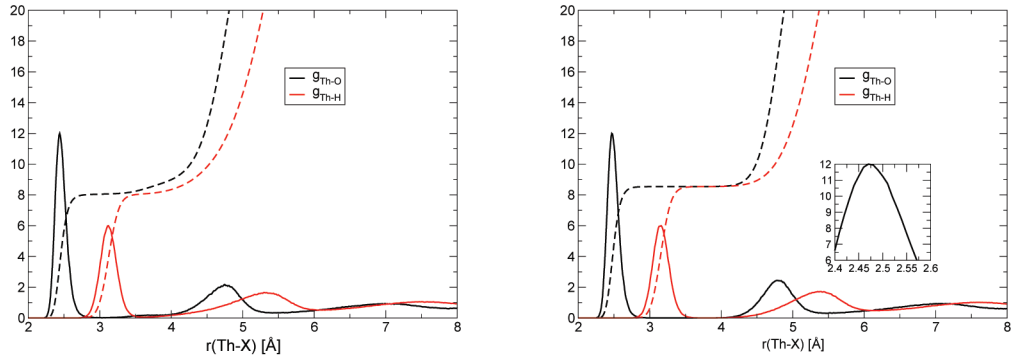

Figure 7. Radial distribution functions $g_{Th-O}(r)$ (black plain line) and $g_{Th-H}(r)$ (red plain line) and their corresponding integrated functions (dashed lines), computed along the trajectories $\mathbf{M}^{TCPEp}_{r_{smooth}=4}$ (a) and $\mathbf{M}^{TCPEp}_{r_{smooth}=7}$ (b).

TABLE 5: Th(IV) Coordination Numbers N_c, Mean Th/Oxygen Distances $\bar{r}_{Th-O}$ in Å, and Probabilities $p(n)$ in Percent of the Various $[Th(H_2O)_n]^{4+}$ Coordination Patterns Computed along the Solvated Trajectories $\mathbf{M}^{TCPEp}_{4,7}$

parameter set	N_c	r(Th−O)	$p(7)$	$p(8)$	$p(9)$	$p(10)$	$p(11)$
$\mathbf{M}^{TCPEp}_4$	8.05	2.44	0.4	91.5	8.1	0.0	0.0
$\mathbf{M}^{TCPEp}_7$	8.45	2.47	0.0	46.1	53.9	0.0	0.0

Å. The $g_{Th-O}(r)$'s thus decrease until reaching a value of zero at about 3 Å, and a second wider peak appears at about 4.75 Å (its height being five to six times smaller than the first one). For the $g_{Th-H}(r)$'s, the same behavior is observed, however, both the latter distances are 3.6 and 5.4 Å. Hence, the radial distribution functions exhibit a well-structured first hydration sphere for Th(IV). From the integrated profiles, the coordination number N_c for Th(IV) is 8.05 and 8.45 along the $\mathbf{M}^{TCPEp}_4$ and $\mathbf{M}^{TCPEp}_7$ trajectories, respectively (See Table 5).

To further analyze the solvation structure of Th(IV), we have computed the instantaneous number N^t_w of water molecules belonging to the Th(IV) first hydration sphere each 500 fs along both types of trajectories. N^t_w corresponds to the number of water molecules whose Th/oxygen distance is smaller than 3.6 Å. The distribution functions of N^t_w reported in Table 5 show that two dominant coordination structures of Th(IV) (made of 8 and 9 water molecules) are observed along the trajectories. Along the $\mathbf{M}^{TCPEp}_4$ ones, a coordination pattern of eight water molecules is mainly observed (it represents 91.5% of the computed structures), whereas the second pattern observed is made of nine molecules (8% of the computed structures), and a pattern of seven molecules may be observed, however, with a small probability of 3.3%. Along the trajectories $\mathbf{M}^{TCPEp}_7$, the N^t_w statistic is strongly altered compared to the latter trajectories; a coordination pattern of nine molecules is now favored (its probability being about 54%), whereas the probability to observe a coordination number of eight is of 46% (note that 7, 10, and 11 coordination numbers are scarcely existing, See Table 5). Hence, along the $\mathbf{M}^{TCPEp}_7$ ones an equilibrium exists between eight and nine Th(IV) coordination patterns, echoing in the two shoulders observed for the first $g_{Th-O}(r)$ peak (located respectively at 2.47 and 2.50 Å, see Figure 7).

In our theoretical framework, the solvation structure of Th(IV) appears thus to strongly depend on the force-field parameters handling the charge-transfer cooperativity (in particular, r_{smooth}). The results obtained with $r_{smooth} = 4$ Å and $r_{smooth} = 7$ Å allows us to estimate lower and upper bounds of the uncertainty affecting our charge transfer term. As discussed previously, while $r_{smooth} = 4$ Å the contribution of the second sphere to the cooperative term is ignored, with $r_{smooth} = 7$ Å the second shell is responsible for 10% of the charge transfer cooperative character. However, it is not easy to provide firm arguments on the choice of the r_{smooth} value.

It is interesting to note that the computed difference in free energies $\Delta G_{8/9}$ between eight and nine coordination patterns are small; about −1.4 and 0.1 kcal mol^{-1} along the trajectories $\mathbf{M}^{TCPEp}_4$ and $\mathbf{M}^{TCPEp}_7$, respectively (the $\Delta G_{8/9}$ are here computed from the above probabilities according to a Boltzmann relation). It is noteworthy that in gas phase, the relative electronic energies (which is in gas-phase a good approximation of the relative free energy[95]) between these two coordination patterns was slightly larger, −4 kcal mol^{-1}, thus indicating that the presence of the water solvent tends to stabilize by 3−4 kcal mol^{-1} the nine-coordinated species with respect to the eight-coordinated one. This trend matches the observed tendency of solvent effects to stabilize higher coordination numbers,[18,96] simply because the larger the number of water molecules, the larger the number of hydrogen bonds to the outer-solvation shells.

Whatever the parameter set considered, our virtual experiments show that the coordination of Th(IV) in aqueous solution lies within 8 and 9, with an average Th/oxygen distance of 2.45 ± 0.02 Å. This result is in excellent agreement with the most recent experimental data of Torapava et al.,[6] who analyzed EXAFS and LAXS spectra and concluded that the first hydration shell is located at a distance of 2.45−2.46 Å. From this value, they argued that nine water molecules belong to the Th(IV) first coordination sphere. However, the latter authors concluded that the experimental uncertainty concerning of the coordination number N_c of Th(IV) is about 10%. Hence, N_c values included within 8 and 10 can also be proposed to interpret their experimental data.

As discussed above, our theoretical $g_{Th-O}(r)$'s exhibit a wider second peak lying within 4 and 5.5 Å (and centered at about 4.75 Å), which corresponds to a partially ordered second hydration sphere. From the integrated $g_{Th-O}(r)$ profiles, we estimate the number of second-sphere water molecules to be 17.5 ± 0.5, which is in very good agreement with the estimate derived from LAXS experiment corresponding to the most diluted conditions, about 18.[6] However, LAXS data suggest the second hydration sphere to be centered at a slightly shorter Th/oxygen distance (about 4.60 ± 0.05 Å) than the one predicted by our simulations.

Conclusions

In this work, we investigated the solvation of Th(IV) in aqueous solution using classical molecular dynamics simulations based on polarizable force-field approaches, which also explicitly

treat the covalent character of the metal/water interaction. It has to be noted that our modeling approach considers a many-body charge-transfer energy term to treat the latter interaction, whereas all the modeling approaches proposed so far consider only additive potentials.

All ion/water force-field parameters are derived from high level ab initio quantum chemical computations (at the MRCI+DC level for studying the Th(IV)/water dimer, and at the MP2 level with large basis sets for larger clusters). We exhibit also that wave function theory methods (such as the MP2 level) combined with large basis sets are more suited than density functional theory methods to study Th(IV)/water aggregates in gas phase. Concerning the model accuracy, the cooperative character of our charge-transfer energy term is pivotal to accurately describe large Th/water clusters; we show that additive approaches can lead to differences up to 100 kcal mol^{-1} concerning the binding energies of 10-coordinated Th/water clusters, as compared to MP2 estimates.

The information extracted from 10 ns solvated trajectories shows a Th(IV) well-structured first hydration shell located at about 2.45 Å and formed of 8−9 water molecules and a second shell at about 4.75 Å and made of 17−18 water molecules. These results are in very good agreement with the most recent experiment and show the predictable character of the proposed approach, which will be used for a systematic study of actinide ions, such as other tetravalent ions, and curium(III).

Acknowledgment. This study was supported by a joint project (JRP 06-11) of the EC-supported ACTINET Network of Excellence. F.R. acknowledges a fellowship from the ACTINET network of excellence. Laboratoire de Physique des Lasers, Atomes et Molécules is Unité Mixte de Recherche Mixte du CNRS. Most of the computations were performed on the large scale facilities of the "Centre de Calcul et de Recherche Technologique" (CCRT) of the French Nuclear Agency (CEA). Additional computational resources have also been provided by the "Institut de Développement et de Ressources en Informatique Scientifique du Centre National de la Recherche Scientifique" (IDRIS-CNRS, contract 71859) and by the "Centre Informatique National de l'Enseignement Supérieur" (CINES, Project phl2531). Michael Trumm and Bernd Schimmelpfennig acknowledge access to the computing resources provided by the Steinbuch Centre for Computing (SCC) at KIT.

References and Notes

(1) *The Chemistry of the Actinide and Transactinide Elements*, 3rd ed.; Morss, L. R., Edelstein, N. M., Fuger, J., Eds.; Springer: Dordrecht, The Netherlands, 2006.
(2) Vallet, V.; Szabó, Z.; Grenthe, I. *Dalton Trans.* **2004**, 3799–3807.
(3) Szabó, Z.; Toraishi, T.; Vallet, V.; Grenthe, I. *Coord. Chem. Rev.* **2006**, *250*, 784–815.
(4) Moll, H.; Denecke, M. A.; Jalilehvand, F.; Sandström, M.; Grenthe, I. *Inorg. Chem.* **1999**, *38*, 1795–1799.
(5) Hennig, C.; Schmeide, K.; Brendler, V.; Moll, H.; Tsushima, S.; Scheinost, A. C. *Inorg. Chem.* **2007**, *46*, 5882–5892.
(6) Torapava, N.; Persson, I.; Eriksson, L.; Lundberg, D. *Inorg. Chem.* **2009**, *48*, 11712–11723.
(7) Rothe, J.; Denecke, M. A.; Neck, V.; Müller, R.; Kim, J. I. *Inorg. Chem.* **2002**, *41*, 249–258.
(8) Johansson, G.; Magini, M.; Ohtaki, H. *J. Sol. Chem.* **1991**, *20*, 775–792.
(9) Johansson, G. Structure of Complexes in Solution Derived from X-Ray Diffraction Measurements. In *Advances in Inorganic Chemistry*; Sykes, A. G., Ed.; Academic Press: London, 1992; Vol. 39.
(10) Fratiello, A.; Lee, R. E.; Schuster, R. E. *Inorg. Chem.* **1970**, *9*, 391–392.
(11) Wilson, R. E.; Skanthakumar, S.; Burns, P. C.; Soderholm, L. *Angew. Chem., Int. Ed.* **2007**, *46*, 8043–8045.
(12) Tsushima, S.; Yang, T.; Mochizuki, Y.; Okamoto, Y. *Chem. Phys. Lett.* **2003**, *375*, 204–212.
(13) Yang, T.; Tsushima, S.; Suzuki, A. *J. Phys. Chem. A* **2001**, *105*, 10439–10445.
(14) Yang, T.; Tsushima, S.; Suzuki, A. *J. Solid State Chem.* **2003**, *171*, 235–241.
(15) Born, M. *Z. Phys.* **1920**, *1*, 45.
(16) Barone, V.; Cossi, M. *J. Phys. Chem. A* **1998**, *102*, 1995–2001.
(17) Barone, V.; Cossi, M.; Tomasi, J. *J. Chem. Phys.* **1997**, *107*, 3210–3221.
(18) Gutowski, K. E.; Dixon, D. A. *J. Phys. Chem. A* **2006**, *110*, 8840–8856.
(19) Wåhlin, P.; Schimmelpfennig, B.; Wahlgren, U.; Grenthe, I.; Vallet, V. *Theor. Chem. Acc.* **2009**, *124*, 377–384.
(20) Car, R.; Parrinello, M. *Phys. Rev. Lett.* **1985**, *55*, 2471–2474.
(21) Bühl, M.; Schreckenbach, G.; Sieffert, N.; Wipff, G. *Inorg. Chem.* **2009**, *48*, 9977–9979.
(22) Rotzinger, F. P. *J. Phys. Chem. B* **2005**, *109*, 1510–1527.
(23) Rotzinger, F. P. *Chem. Rev.* **2005**, *105*, 2003–2038.
(24) Cao, Z.; Balasubramanian, K. *J. Chem. Phys.* **2005**, *123*, 114309.
(25) (a) Rotzinger, F. P. *Chem.—Eur. J.* **2007**, *13*, 800–811. (b) Vallet, V.; Wahlgren, U.; Grenthe, I. *Chem.—Eur. J.* **2007**, *13*, 10294–10297. (c) Rotzinger, F. P. *Chem.—Eur. J.* **2007**, *13*, 10298–10302.
(26) Wåhlin, P.; Danilo, C.; Vallet, V.; Réal, F.; Flament, J.-P.; Wahlgren, U. *J. Chem. Theory Comput.* **2008**, *4*, 569–577.
(27) Austin, J. P.; Burton, N. A.; Hillier, I. H.; Sundararajan, M.; Vincent, M. A. *Phys. Chem. Chem. Phys.* **2009**, *11*, 1143–1145.
(28) Zhao, Y.; Truhlar, D. G. *Theor. Chem. Acc.* **2008**, *120*, 215–241.
(29) Hofer, T. S.; Scharnagl, H.; Randolf, B. R.; Rode, B. M. *Chem. Phys.* **2006**, *327*, 31–42.
(30) Frick, R. J.; Pribil, A. B.; Hofer, T. S.; Randolf, B. R.; Bhattacharjee, A.; Rode, B. M. *Inorg. Chem.* **2009**, *48*, 3993–4002.
(31) Merabet, M.; Bose, T. K. *J. Phys. Chem.* **1988**, *92*, 6149–6150.
(32) Nandi, N.; Bhattacharyya, K.; Bagchi, B. *Chem. Rev.* **2000**, *100*, 2013–2046.
(33) Bagchi, B. *Chem. Rev.* **2005**, *105*, 3197–3219.
(34) Guilbaud, P.; Wipff, G. *J. Mol. Struct.* **1996**, *366*, 55–63.
(35) Hutschka, F.; Dedieu, A.; Troxler, L.; Wipff, G. *J. Phys. Chem. A* **1998**, *102*, 3773–3781.
(36) Yang, T.; Bursten, B. E. *Inorg. Chem.* **2006**, *45*, 5291–5301.
(37) Hemmingsen, L.; Amara, P.; Ansorborlo, E.; Field, M. J. *J. Phys. Chem. A* **2000**, *104*, 4095–4101.
(38) Clavaguéra-Sarrio, C.; Brenner, V.; Hoyau, S.; Marsden, C. J.; Millié, P.; Dognon, J.-P. *J. Phys. Chem. B* **2003**, *107*, 3051–3060.
(39) Clavaguéra, C.; Sansot, E.; Calvo, F.; Dognon, J.-P. *J. Phys. Chem. B* **2006**, *110*, 12848–12851.
(40) Clavaguéra, C.; Calvo, F.; Dognon, J.-P. *J. Chem. Phys.* **2006**, *124*, 074505.
(41) Hagberg, D.; Karlström, G.; Roos, B. O.; Gagliardi, L. *J. Am. Chem. Soc.* **2005**, *127*, 14250–14256.
(42) Hagberg, D.; Bednarz, E.; Edelstein, N. M.; Gagliardi, L. *J. Am. Chem. Soc.* **2007**, *129*, 14136–14137.
(43) Galbis, E.; Hernández-Cobos, J.; den Auwer, C.; Le Naour, C.; Guillaumont, D.; Simoni, E.; Papparlardo, R. R.; Sánchez Marcos, E. *Angew. Chem., Int. Ed.* **2010**, *49*, 3811–3815.
(44) García-Hernandez, M.; Lauterbach, C.; Krüger, S.; Matveev, A.; Rösch, N. *J. Comput. Chem.* **2002**, *23*, 834–846.
(45) Douglas, M.; Kroll, N. M. *Ann. Phys.* **1974**, *82*, 89–155.
(46) Hess, B. A. *Phys. Rev. A* **1986**, *33*, 3742–3748.
(47) Roos, B. O.; Lindh, R.; Malmqvist, P.-Å.; Veryazov, V.; Widmark, P.-O. *J. Phys. Chem. A* **2004**, *108*, 2851–2858.
(48) Roos, B. O.; Lindh, R.; Malmqvist, P.-Å.; Veryazov, V.; Widmark, P.-O. *Chem. Phys. Lett.* **2005**, *409*, 295–299.
(49) Dirac, P. A. M. *Proc. R. Soc. London, Ser. A* **1929**, *123*, 714–733.
(50) Slater, J. C. *Phys. Rev.* **1951**, *81*, 385–390.
(51) Becke, A. D. *Phys. Rev. A* **1988**, *38*, 3098–3100.
(52) Vosko, S. H.; Wilk, L.; Nusair, M. *Can. J. Phys.* **1980**, *58*, 1200–1211.
(53) (a) Perdew, J. P. *Phys. Rev. B* **1986**, *33*, 8822–8824. (b) Perdew, J. P. *Phys. Rev. B* **1986**, *34*, 7406–7406.
(54) Lee, C.; Yang, W.; Parr, R. G. *Phys. Rev. B* **1988**, *37*, 785–789.
(55) Becke, A. D. *J. Chem. Phys.* **1993**, *98*, 5648–5652.
(56) Hampel, C.; Peterson, K. A.; Werner, H.-J. *Chem. Phys. Lett.* **1992**, *190*, 1–12.
(57) Langhoff, S. R.; Davidson, E. R. *Int. J. Quantum Chem.* **1974**, *8*, 61–72.
(58) Werner, H.-J.; Knowles, P. J. *J. Chem. Phys.* **1988**, *89*, 5803–5814.
(59) Knowles, P. J.; Werner, H.-J. *Chem. Phys. Lett.* **1988**, *145*, 514–522.
(60) Werner, H.-J.; et al. *MOLPRO*, version 2006.1, a package of ab initio programs; 2006; see http://www.molpro.net.
(61) Karlström, G.; Lindh, R.; Malmqvist, P.-Å.; Roos, B. O.; Ryde, U.; Veryazov, V.; Widmark, P.-O.; Cossi, M.; Schimmelpfennig, B.; Neogrady, P.; Seijo, L. *Comput. Mater. Sci.* **2003**, *28*, 222–239.
(62) Boys, S. F.; Bernardi, F. *Mol. Phys.* **1970**, *19*, 553–566.

(63) Deleted in proof.
(64) Deleted in proof.
(65) Deleted in proof.
(66) Stevens, W. J.; Fink, W. *Chem. Phys. Lett.* **1987**, *139*, 15–22.
(67) Schmidt, M. W.; Baldridge, K. K.; Boatz, J. A.; Elbert, S. T.; Gordon, M. S.; Jensen, J. J.; Koseki, S.; Matsunaga, N.; Nguyen, K. A.; Su, S.; Windus, T. K.; Dupuis, M.; Montgomery, J. A. *J. Comput. Chem.* **1993**, *14*, 1347–1363.
(68) Küchle, W.; Dolg, M.; Stoll, H.; Preuss, H. *J. Chem. Phys.* **1994**, *100*, 7535–7542.
(69) Cao, X.; Dolg, M. *J. Mol. Struct. (THEOCHEM)* **2004**, *673*, 203–209.
(70) Dunning, T. H., Jr. *J. Chem. Phys.* **1989**, *90*, 1007–1023.
(71) Weigend, F.; Häser, F. *Theor. Chim. Acta* **1997**, *97*, 331–340.
(72) Weigend, F.; Häser, F.; Patzelt, H.; Ahlrichs, R. *Chem. Phys. Lett.* **1998**, *294*, 143–152.
(73) *TURBOMOLE V6.1 2009*, a development of University of Karlsruhe and Forschungszentrum Karlsruhe GmbH, 1989−2007, TURBOMOLE GmbH, since 2007; available from http://www.turbomole.com.
(74) Kumar, R.; Wang, F.-F.; Jenness, G. R.; Jordan, K. D. *J. Chem. Phys.* **2010**, *132*, 014309.
(75) Cieplak, P.; Dupradeau, F.-Y.; Duan, Y.; Wang, J. *J. Phys.: Condens. Matter* **2009**, *21*, 333102.
(76) Masella, M.; Flament, J.-P. *J. Chem. Phys.* **1997**, *107*, 9105–9116.
(77) Caldwell, J.; Dang, L.; Kollman, P. *J. Am. Chem. Soc.* **1990**, *112*, 9144–9147.
(78) Masella, M.; Cuniasse, P. *J. Chem. Phys.* **2003**, *119*, 1866–1873.
(79) Masella, M.; Flament, J.-P. *J. Chem. Phys.* **1999**, *111*, 5081–5090.
(80) Masella, M.; Borgis, D.; Cuniasse, P. *J. Comput. Chem.* **2008**, *29*, 1707–1724.
(81) Masella, M.; Gresh, N.; Flament, J.-P. *J. Chem. Soc., Faraday Trans.* **1998**, *94*, 2745–2753.
(82) Tschumper, G. S.; Leininger, M. L.; Hoffman, B. C.; Valeev, E. F.; Schaefer, H. F.; Quack, M. *J. Chem. Phys.* **2002**, *116*, 690–701.
(83) Houriez, C.; Ferré, N.; Masella, M.; Siri, D. *J. Chem. Phys.* **2008**, *128*, 244504.
(84) *Handbook of Atomic Data*; Fraga, S., Karwowski, J., Saxena, K. M. S., Eds.; Elsevier: Amsterdam, 1976.
(85) Fowler, P. W.; Harding, J. H.; Pyper, N. C. *J. Phys.: Condens. Matter* **1994**, *6*, 10593–10606.
(86) Shannon, R. D.; Fischer, R. X. *Phys. Rev. B* **2006**, *73*, 235111.
(87) Réal, F.; Vallet, V.; Clavaguéra, C.; Dognon, J.-P. *Phys. Rev. A* **2008**, *78*, 052502.
(88) Masella, M. *Mol. Phys.* **2006**, *104*, 415–428.
(89) Doherty, J. PEST: Model-Independent Parameter Estimation and Uncertainty Analysis, 2010; see http://www.pesthomepage.org.
(90) Liu, Y.; Tuckerman, M. E. *J. Chem. Phys.* **2000**, *112*, 1685–1700.
(91) Smith, W. *CCP5 Inf. Q.* **1982**, *4*, 13.
(92) Martyna, G. J.; Tuckerman, M. E.; Tobias, D. J.; Klein, M. L. *Mol. Phys.* **1996**, *87*, 1117–1157.
(93) Sandström, M.; Persson, I.; Jalilehvand, F.; Lindqvist-Reis, P.; Spångberg, D.; Hermansson, K. *J. Synchrotron Rad.* **2001**, *8*, 657–659.
(94) Ciupka, J.; Cao-Dolg, X.; Wiebke, J.; Dolg, M. *Phys. Chem. Chem. Phys.* **2010**, *12*, 13215−13223.
(95) Vallet, V.; Wahlgren, U.; Grenthe, I. *J. Am. Chem. Soc.* **2003**, *125*, 14941–14950.
(96) Vallet, V.; Wahlgren, U.; Schimmelpfennig, B.; Szabó, Z.; Grenthe, I. *J. Am. Chem. Soc.* **2001**, *123*, 11999–12008.

JP108061S